



Semi-automated impact device based on human behaviour recognition model for in-service modal analysis

Fahad Bin Zahid¹ · Zhi Chao Ong¹ · Shin Yee Khoo¹ · Mohd Fairuz Mohd Salleh²

Received: 24 December 2021 / Accepted: 4 January 2023

© The Author(s), under exclusive licence to The Brazilian Society of Mechanical Sciences and Engineering 2023

Abstract

Modal analysis is a reliable method for the study of structural behaviour. A novel modal analysis technique called impact synchronous modal analysis (ISMA) was developed using which modal analysis can be performed in the presence of ambient forces. However, studies determined that the manual operation of this technique is laborious, time intensive and has limited practicality due to the lack of control and knowledge of the impact with respect to the phase angle of the disturbances using conventional impact hammer. A fully automated impact device called automated phase controlled impact device (APCID) was developed to perform in-service modal analysis with minimum number of impacts. However, large size and heavy weight of this device made it unsuitable for real world applications. In this paper, a portable semi-automated impact device is used to perform in-service modal analysis. The device uses the conventional manual impact hammer and is equipped with inertial measurement unit (IMU). It is operated manually and uses human behaviour recognition along with control of APCID which gives indication to impart impact based on human's physical behaviour. This physical behaviour is recognized by classifying different impact types and predicting impact times using machine learning technique from the inertial sensor data. The cyclic load components at 20 Hz and 30 Hz are reduced by 91.2% and 92.5%, respectively, using the proposed ISMA with IMU. The extracted modal parameters are also in good correlation with the benchmark, experimental modal analysis data as well as the previous work using APCID. All the modes are identified with less than 3% difference in natural frequencies, less than 10% difference in damping values and modal assurance criterion values greater than 0.9 for all modes at running frequencies of 20 Hz and 30 Hz.

Keywords APCID · ISMA · Human behaviour recognition · Semi-automated impact device · Modal analysis · Machine learning

1 Introduction

Vibration is the root cause of many mechanical failures. Such failures can be avoided if dynamic properties of a structure are known. Modal analysis is a frequently used technique to obtain dynamic characteristics of a structure.

Three parameters namely natural frequencies, mode shapes and damping ratios can comprehensively define dynamic characteristics of a structure [1]. Various engineering systems can be described through these modal parameters to identify and understand the main cause of vibration problems. Modal analysis is being used in a number of applications like troubleshooting, load estimation, validation of Finite Element (FE) model, sensitivity analysis, Structural Health Monitoring (SHM), damage detection, substructure coupling, quantifying and locating damage etc. [1–7].

Two commonly used modal analysis techniques are Experimental Modal Analysis (EMA) [8] and Operational Modal Analysis (OMA) [9, 10]. In EMA, known impact force is used to excite the system and the system needs to be in non-operating condition to avoid any unaccounted force. However, system shutdown can be very costly in terms of production losses especially in industries like petrochemical,

Technical Editor: Samuel da Silva.

✉ Zhi Chao Ong
alexongzc@um.edu.my; zhichao83@gmail.com

¹ Department of Mechanical Engineering, Faculty of Engineering, Universiti Malaya, 50603 Kuala Lumpur, Malaysia

² SD Advance Engineering, 7-5, Pusat Dagangan UMNO Shah Alam, Lot 8, Persiaran Damai, Seksyen 11, 40100 Shah Alam, Selangor Darul Ehsan, Malaysia

oil and gas industries making EMA an unpractical solution for such cases. Moreover, using EMA, the system cannot be tested under real operating conditions. To avoid such situations, where production losses are high, the structure under testing is too large to be excited artificially or structure need to be tested under real operating conditions, OMA is used. OMA provides certain benefits over EMA when it comes to practicality and user-friendliness. OMA uses ambient excitation instead of artificial excitation as the system input and it is performed under actual operating conditions. However, the modal parameters extracted using OMA are affected by the absence of known input forces as mode shapes obtained from OMA cannot be normalized accurately, subsequently affecting the mathematical models for further analysis purposes [11].

A novel modal analysis technique called Impact Synchronous Modal Analysis (ISMA) was introduced [12, 13] to address the limitations of EMA and OMA. ISMA uses known input excitation and structures can be tested under their actual operation. Previous studies have shown that ISMA has been used successfully to obtain modal parameters in rotor and structural dynamic systems during their actual operation [13, 14]. ISMA requires sufficient number of impacts in order to average out and suppress all the unaccounted forces [15]. For improved efficiency of ISMA, the impact responses and cyclic load components should be out of phase. Studies have shown that 4 averages can be

sufficient to remove disturbances when they are out of phase with respect to the impact response for every applied impact [16]. From these studies, it was concluded that ISMA's manual operation is laborious and time intensive (i.e., requires hundreds of averages).

In an attempt to rectify the problems of ISMA's manual operation, an automated impact device called Automated Phase Controlled Impact Device (APCID) was developed to remove cyclic load components with least number of averages by feeding the phase angle information of responses from cyclic load back to the device [17–19]. Using APCID, impacts can be applied at the desired time which is always out of phase with respect to the phase of response from cyclic load. APCID uses a counter as an indication of when to impart impact and counter's time interval $T_{counter}$ is determined by Eq. (1) [18]

$$T_{counter} = T_{\varnothing} + T_{cycle} + T_{desired} - T_{lag} - T_{offset} \quad (1)$$

where T_{\varnothing} is the phase difference time, T_{cycle} is time interval of the load cycles, $T_{desired}$ is time interval of the desired impact, T_{lag} is the time lag and T_{offset} is time taken by the impact device to impart impact after getting the signal [18].

In ISMA, Impact Synchronous Time Averaging (ISTA) [13] is used before performing the Fast Fourier Transform (FFT) to filter out all the unknown responses in the time domain, leaving only impact device's response. Using

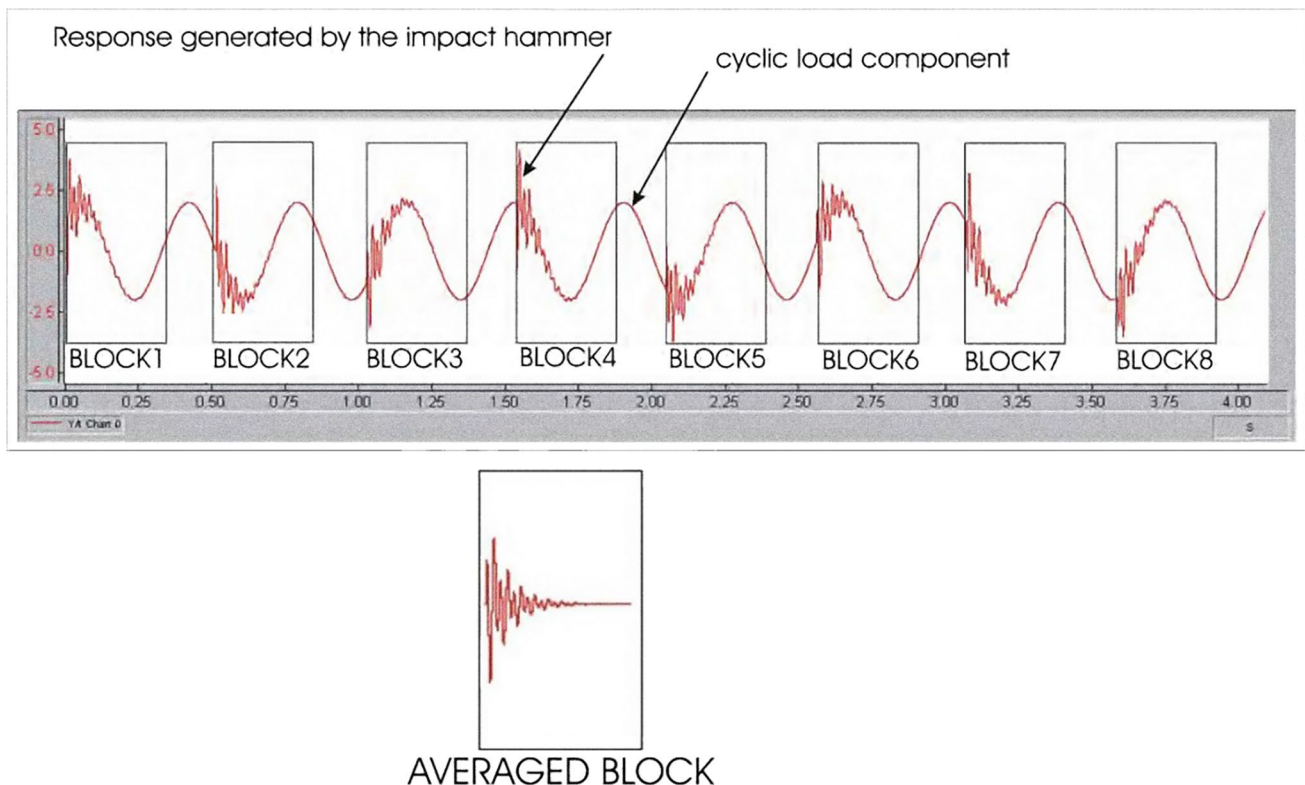


Fig. 1 Elimination of running speed with ISTA [12]

Fig. 2 Test rig with measurement points (black circles)

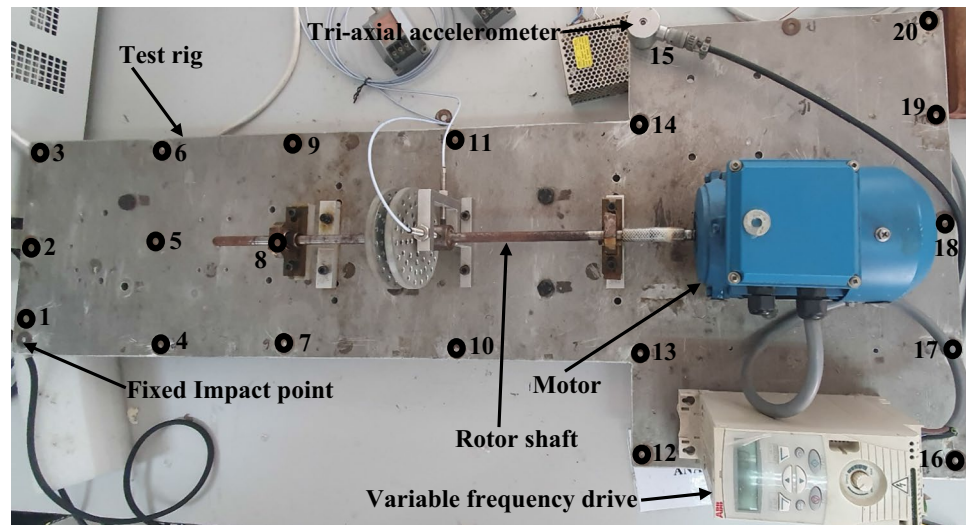
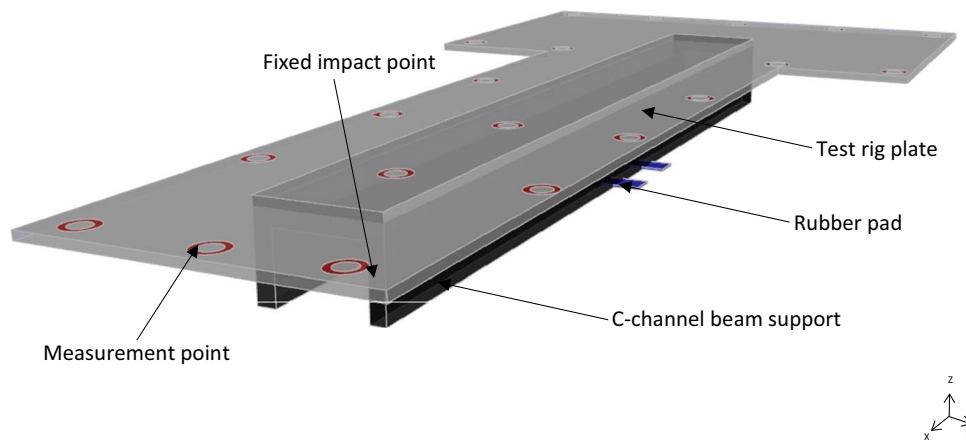


Fig. 3 Schematic view of the test rig in simply supported boundary condition



ISMA, the responses from unaccounted disturbances are eliminated even if they have the same frequency component as that contained in the impulse response when the phase of disturbance is not consistent with respect to the impact.

In ISTA, impact force signal is used as reference to trigger acquisition of the time block. Random noises and harmonic disturbances are filtered out by performing block averaging on both the impact force signal and response signal due to impact for each acquired time block and by taking adequate number of averages. As the random noises and harmonic disturbances filters out, only the response due to impact is left behind. Effect of ISTA in eliminating cyclic load component is shown in Fig. 1 [12].

Studies show that if consecutive impacts are applied at 180 degrees out of phase, i.e., crest–trough–crest–trough, the cyclic load component can be removed with as low as 4 averages [16, 20]. Using APCID for performing ISMA, cyclic load component can be removed with least number of averages by imparting consecutive impacts at nearly 180 degrees out of phase.

Although APCID resolve problems associated with manual operation of ISMA, however its practicality for commercial use is limited. The impact device, its power supply and its support structure used in APCID makes it large, heavy and unsuitable for commercial use. To fix this problem, the mechanical actuator in APCID can be replaced with human hand to impart impact while still using the control scheme of APCID. However, the accuracy of the control scheme of APCID can be seriously affected by the inherited randomness in human behaviour. When using APCID, time taken by the impact device to impart impact after getting signal (T_{offset}) is consistent but with manual operation, T_{offset} would be random. This randomness would lead to the problems associated with manual operation of ISMA, which lead to the development of APCID. However, human behaviour can be studied by monitoring human motions using Inertial Measurement Unit (IMU) and machine learning can be used to compensate for the randomness in behaviour.

IMUs have been successfully used with machine learning for monitoring and recognizing human motions/behaviour

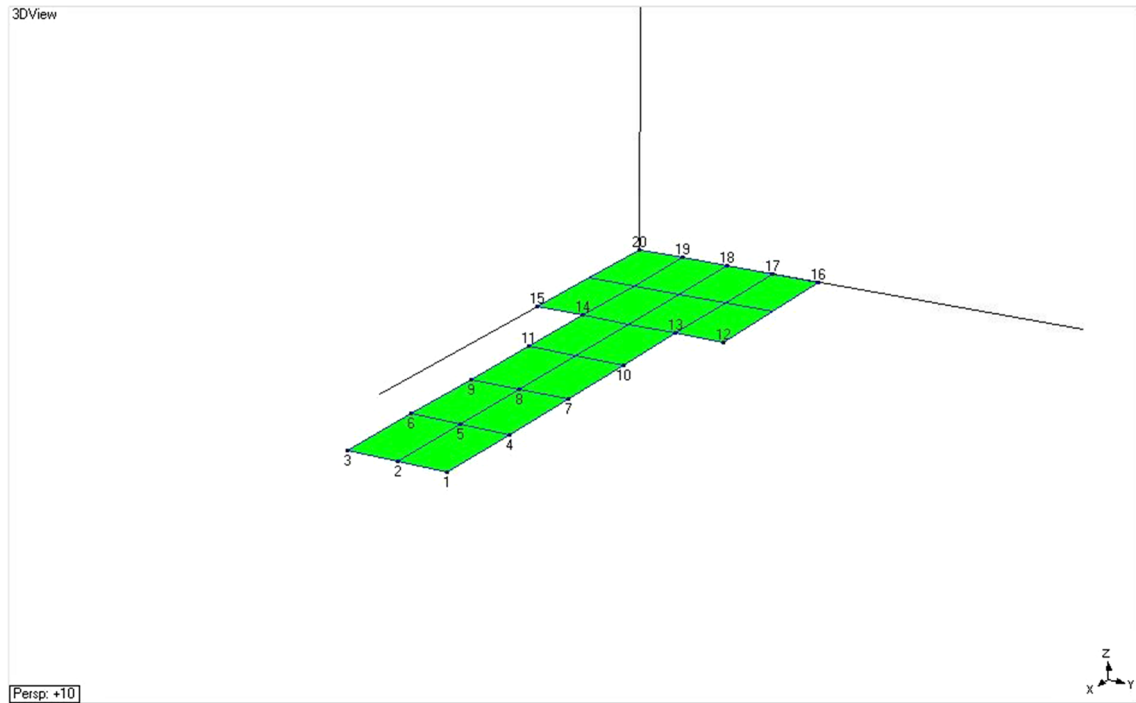


Fig. 4 Structural model of the test rig

Fig. 5 Semi-automated Impact device



[21–23]. In a recent study [24], IMU (BNO055) was used with Back Propagation Artificial Neural Network (BP ANN) to classify 13 different impact types for modal testing and this classification machine learning model was then used to predict impact time/ T_{offset} of impacts during modal testing. The classification model gave 96% accuracy in classifying 13 different types of impacts in real-time modal testing. The study showed that the variation in impact time due to different impact types can be reduced 2 to 3 times by successful impact classification. The time prediction model developed using classification model to compensate for variations of T_{offset} in APCID control represented by Eq. (1) gave mean prediction error of 5.2% compared to measured impact time for 100 impacts in real-time testing.

In an attempt to develop a portable and user-friendly impact device for in-service modal analysis, a semi-automated impact device is used in this paper to perform ISMA at running frequencies of 20 Hz and 30 Hz. Impacts are imparted by human instead of machine and impact time prediction model based on IMU data [24] is used to compensate for variations due to human behaviour in T_{offset} . Results are compared against the Benchmark, EMA performed at stationary condition and ISMA using random impacts, (i.e., impacts imparted randomly without any notification) [12, 13] performed at 20 Hz and 30 Hz. The accuracy of the results is also compared to the accuracy of the results of ISMA performed using APCID, (i.e., ISMA with APCID/fully automated impact device) [18]. The semi-automated impact device using IMU and APCID control scheme represented by Eq. (1) is also referred to as ISMA with IMU in the upcoming sections.

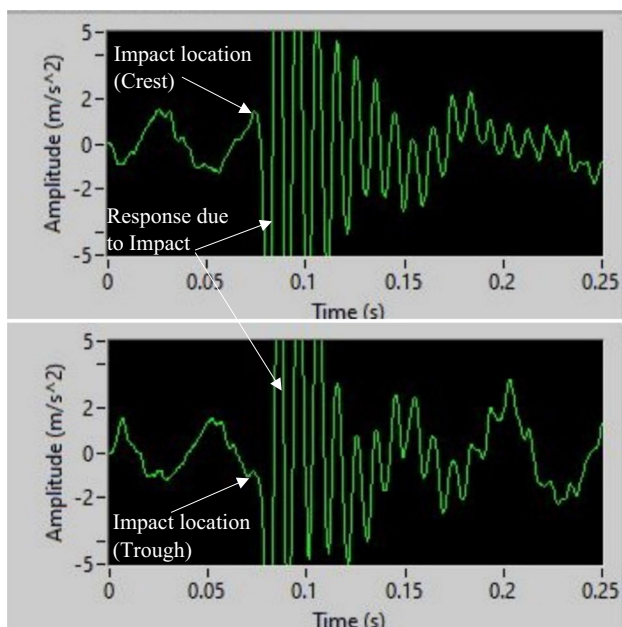


Fig. 6 180 degrees out of phase consecutive impacts (crest and trough)

2 Methodology

2.1 Experimental setup

Figure 2 shows the test structure used for modal testing which is a lab-scale motor driven rotor fault simulation rig. Different machinery faults such as imbalance, misalignment, bearing faults can be simulated and the vibration on the bearing as well as the entire test structure can be analysed as it is usually observed in actual industrial machines. The plate acts as the structural skid of this motor driven loaded rotor. It is bolted on a C-channel beam and the entire test rig is simply supported on rubber pads. Schematic view of the test rig in simply supported boundary condition is shown in Fig. 3. This test rig can represent a typical motor driven machine sitting on the main skid, the modes of interest are those modes falling within the operating frequency range of the driver motor, i.e., 0–50 Hz in this case, for the evaluation of the dynamic design of the entire machine assembly.

Testing was done at 20 Hz and 30 Hz running frequencies of the motor. A roving tri-axial accelerometer (IMI 604B31) was used to get the excitation response at different locations of the test rig by fixing the point of excitation/impact. Excitation measurement points are highlighted with black circles and numbered in Fig. 2. The structural model of the test rig is shown in Fig. 4, where 20 test points/locations are labelled with point 1 being the fixed impact point. The impacts were imparted along z-axis, (i.e., coordinate axes shown in Fig. 4), and response due to impact was recorded with tri-axial accelerometer at each of the 20 points for each test. Excitation force used to excite the structure was 20–60 N and rubber tip was used for the impact hammer.

Figure 5 shows the semi-automated impact device used for this study. The impact hammer (PCB 086C03) is integrated with Arduino Nano and IMU (BNO055) to predict impact time/ T_{offset} based on physical human behaviour using BP ANN machine learning model [24]. The predicted impact time (T_{offset}) used in Eq. (1) was applied in this study to give the indication to the operator to impart impact at the desired location. Arduino Nano acquired data from IMU at sampling rate of 100 samples/sec.

The excitation and response signals were acquired using National Instruments NI USB-9234 data acquisition card at sampling rate of 2048 samples/sec. LabVIEW 2013 software was used for signal processing of all the signals. The excitation and response signals were acquired in data blocks with block size of 2 s (4096 samples). ME scope software was used to draw structural model of the test rig and to extract modal parameters. 4096 samples (2 s) of vibration signal were used for post-processing. Frequency Response Functions (FRFs) were obtained from modal testing at the 20 measurement points and the FRFs were overlaid to identify

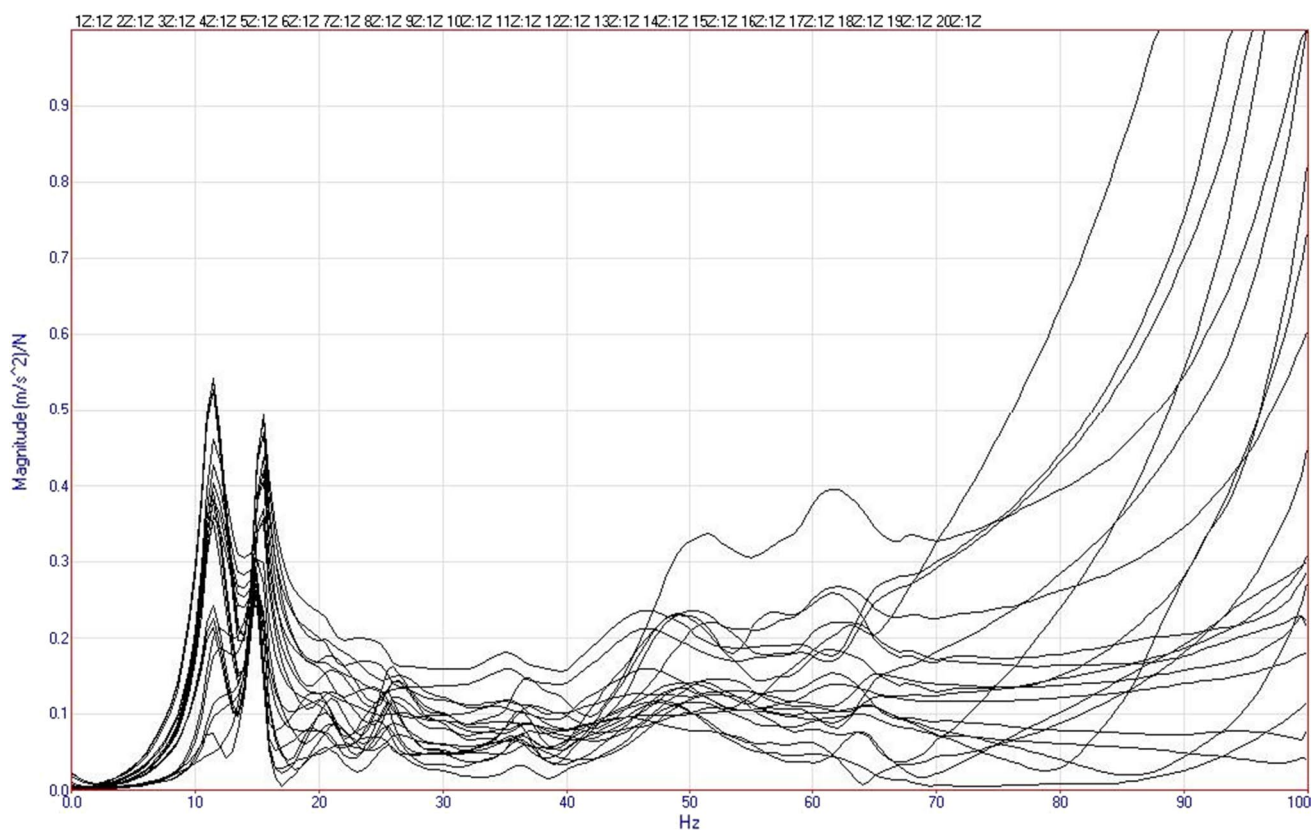


Fig. 7 FRF estimation for EMA using impact hammer (Benchmark)

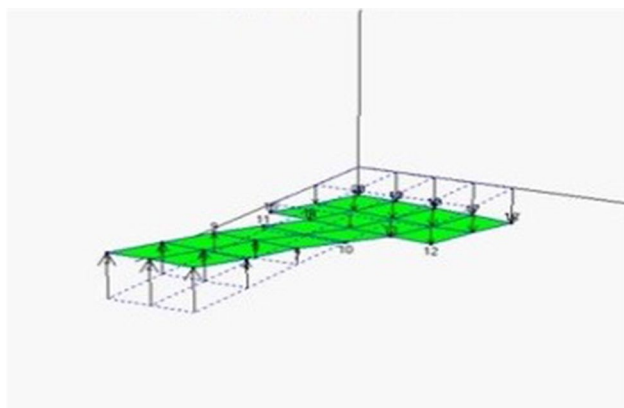


Fig. 8 EMA 1st mode 11.48 Hz

the modes and estimate their respective modal parameters (natural frequencies, damping and mode shapes).

2.2 Testing procedure

EMA was performed at stationary condition of the test rig to use as Benchmark. 5 averages were performed at each point of the test rig for EMA. ISMA using random impacts was performed at 20 Hz and 30 Hz running frequencies of

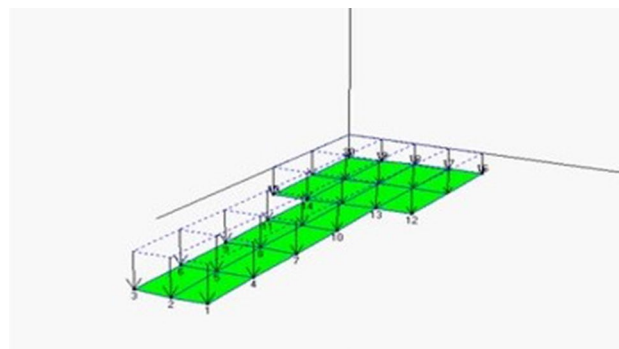


Fig. 9 EMA 2nd mode 15.12 Hz

the motor. In ISMA using random impacts, impacts were imparted randomly like in EMA with random impact locations. 20 averages were performed at each point of the test rig at both 20 Hz and 30 Hz. ISMA with IMU was also performed at 20 Hz and 30 Hz running frequencies of the motor. A LED indicator was used in these tests to notify the operator to impart impact according to the desired impact location. The desired impact locations were set as 180 degrees out of phase for consecutive impacts (crest and trough) [18, 25], so that the running frequency cancel out more efficiently in averaging leaving behind only response due to impact.

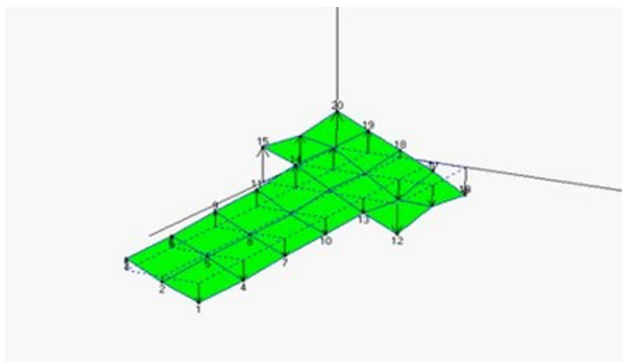


Fig. 10 EMA 3rd mode 25.44 Hz

Figure 6 shows impact locations of consecutive impacts during actual testing followed by the response due to impact. For ISMA with IMU, 10 averages were taken at each point of the test rig for both 20 Hz and 30 Hz of motor running frequency.

The semi-automated impact device uses machine learning models developed in [24] for human behaviour recognition. For impact classification model, impact device orientation data during 13 different types of impacts was used for the development of impact classification machine learning model. The class labels of this model were then used as one of the inputs along with reaction time and maximum impact

speed to predict the impact time (T_{offset}) based on physical human behaviour. The results showed good prediction accuracy with only about 5% of mean error.

3 Results

3.1 Benchmark EMA

Frequency Response Function (FRF) of the Benchmark EMA performed at stationary condition of the test rig is shown in Fig. 7.

In the FRF in Fig. 7, 3 modes can be observed at 11.48 Hz, 15.12 Hz and 25.44 Hz. The mode shapes are given in Figs. 8, 9 and 10.

From Figs. 8, 9 and 10, it can be observed that the 1st mode is pitching, 2nd mode shape is heaving and 3rd mode shape is rolling. Pitching, heaving and rolling are common mode shapes to identify form of vibration of a plate like structure [26–30].

3.2 ISMA at 20 Hz running frequency with random impacts and semi-automated impact device:

ISMA using random impacts was performed at 20 Hz running frequency with 20 averages. The resulting FRF is shown in Fig. 11.

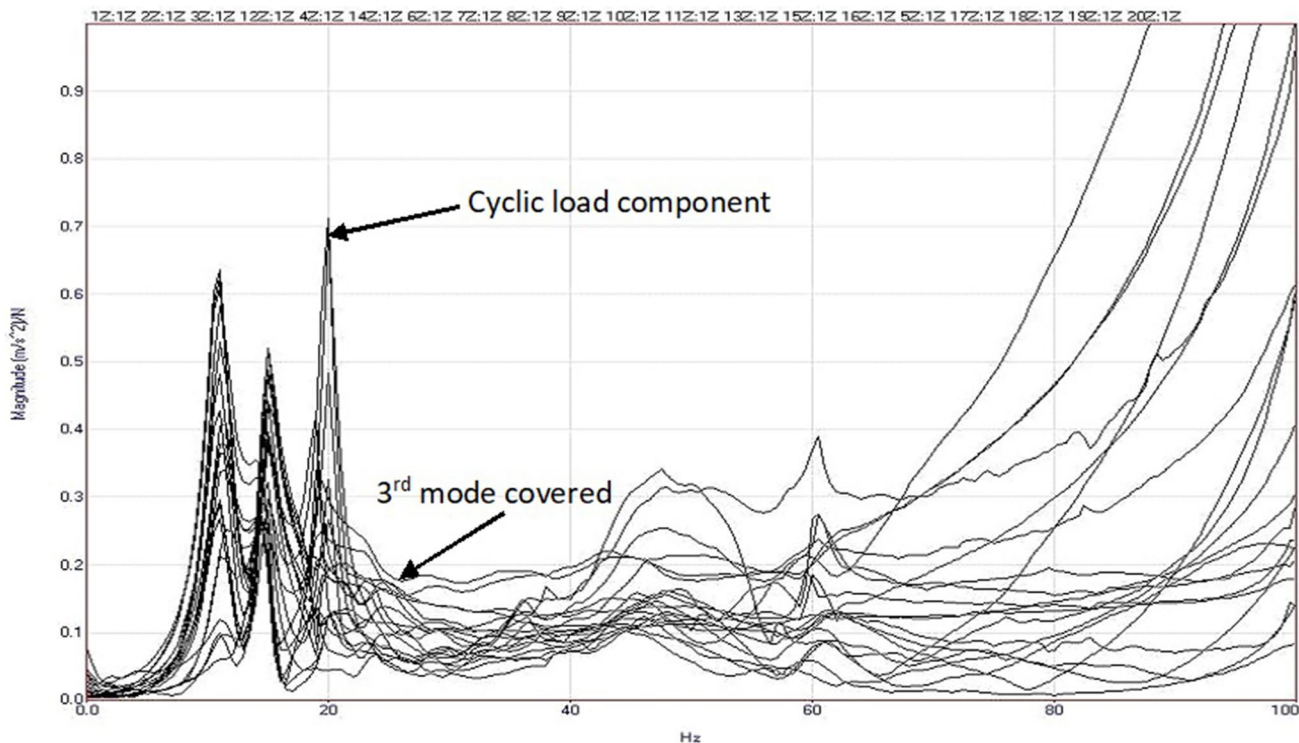


Fig. 11 FRF estimation for ISMA using random impacts at 20 Hz (20 averages)

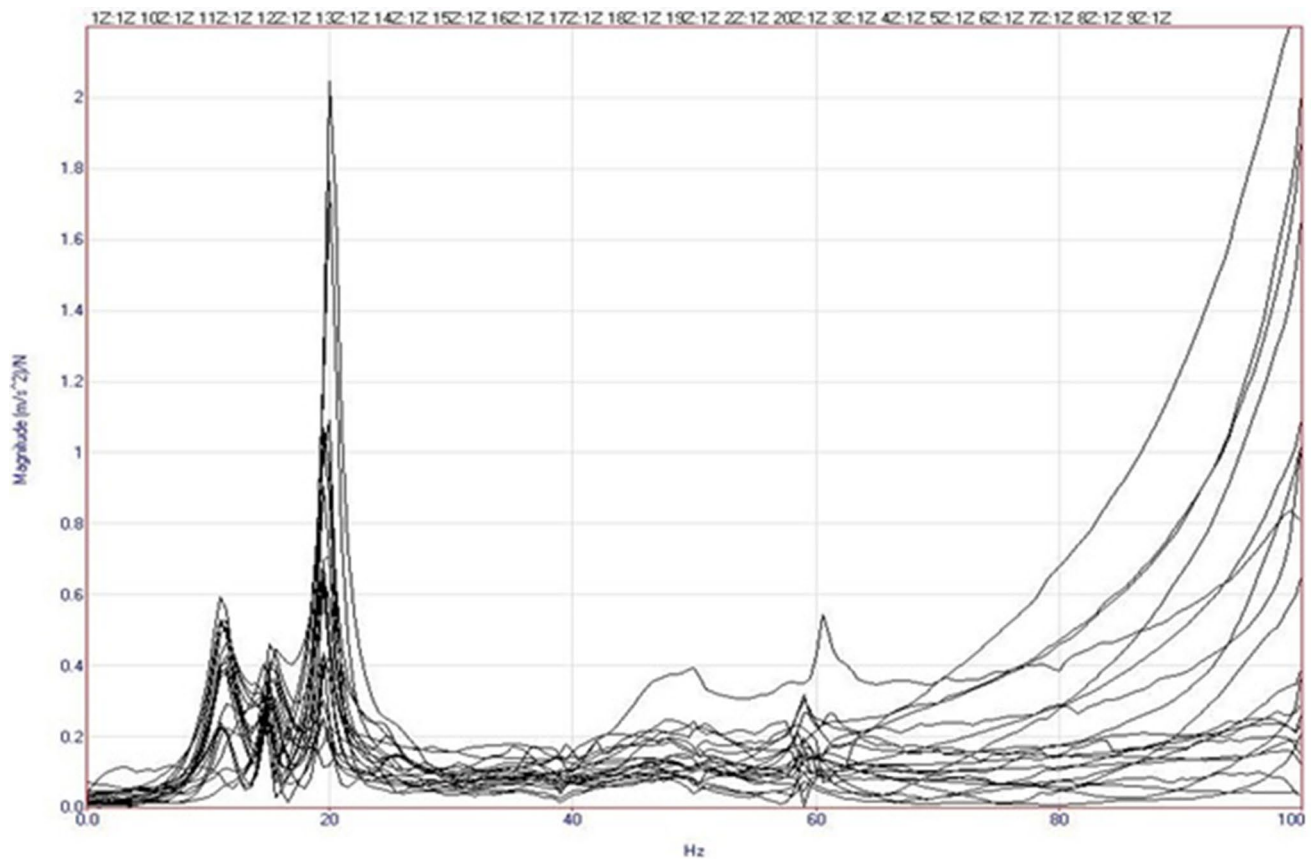


Fig. 12 FRF estimation for ISMA using IMU at 20 Hz (1st average)

Figure 11 shows high amplitude peaks at 20 Hz due to cyclic load component still present after 20 averages. Mode 1 and 2 can be observed similar to EMA at 10.86 Hz and 15.03 Hz, respectively. However, less sensitive 3rd mode cannot be observed because it is covered by cyclic load component.

ISMA was performed at 20 Hz using semi-automated impact device (i.e., ISMA with IMU). The resulting FRFs at 1st average, 4 averages and 10 averages are shown in Figs. 12, 13 and 14, respectively.

Figure 12 shows that 1st and 2nd modes can be observed in the FRF but 3rd mode is covered by the high peaks at 20 Hz due to cyclic load component at the start of the test. Figure 13 shows the FRF after 4 averages and it can be observed that the cyclic load component has been reduced significantly in just 4 averages from 2.05 m/s²N to 0.32 m/s²N with 84.4% suppression and the 3rd mode is starting to show up as the cyclic load component is suppressed. Figure 14 shows the FRF after 10 averages and it can be observed that cyclic load component is almost removed with 91.2% suppression (reduction from 2.05 m/s²N to 0.18 m/s²N), and the 3rd mode can be observed clearly. From Fig. 14, 3 modes can be observed at 11.12 Hz, 14.84 Hz and 24.87 Hz similar

to EMA. From Figs. 11 and 13, it can be observed that the cyclic load component is significantly suppressed with just 4 averages using semi-automated impact device compared to ISMA using random impacts for 20 averages. Mode shapes obtained from semi-automated impact device at 20 Hz after 10 averages are shown in Figs. 15, 16 and 17.

From Figs. 15, 16 and 17, it can be observed that 1st mode shape is pitching, 2nd mode shape is heaving and 3rd mode shape is rolling, similar to the benchmark EMA.

Summary and comparison of the modal parameters extracted from benchmark EMA, ISMA using random impacts at 20 Hz, semi-automated impact device at 20 Hz and ISMA with APCID [18] at 20 Hz is given in Table 1.

Table 1 shows the natural frequencies and damping values of the modes observed in EMA, ISMA using random impacts and ISMA with IMU, (i.e., semi-automated impact device) at 20 Hz of running frequency. Table 2 gives the comparison of the modal parameters with the benchmark EMA in terms of percentage difference and Modal Assurance Criterion (MAC) values of ISMA using random impacts, ISMA with IMU and ISMA with APCID [18] at 20 Hz. The results of the ISMA with APCID were obtained from previous research [18]. Table 2 shows that all the

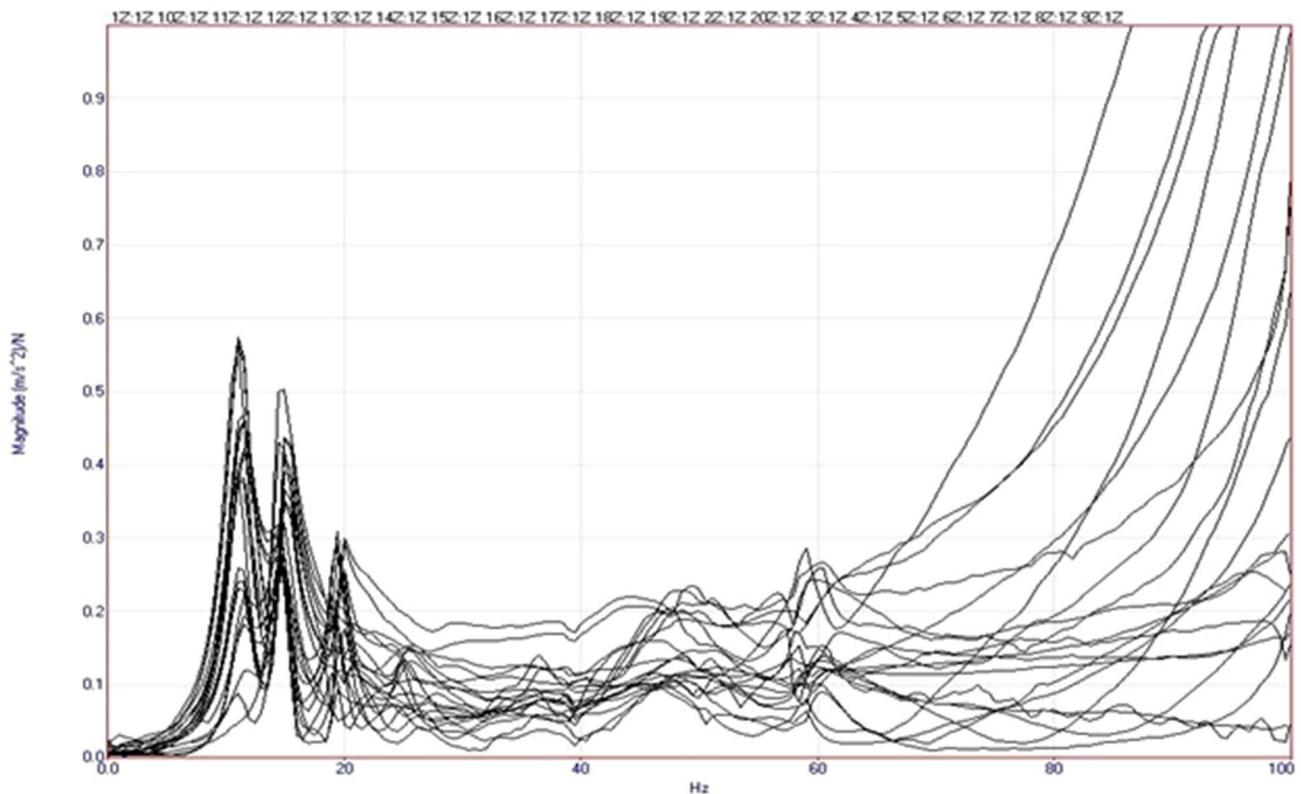


Fig. 13 FRF estimation for ISMA using IMU at 20 Hz (4 averages)

modes estimated in EMA are also estimated in ISMA with IMU with less than 3% difference in natural frequencies and less than 10% difference in damping values for all modes. In ISMA using random impacts, 1st and 2nd modes have natural frequencies close to EMA while 3rd mode is not estimated due to presence of large cyclic load component at 20 Hz. The damping value of the 1st mode is close to EMA, but the damping value of the 2nd mode is a little off with a difference of around 19% compared to EMA. Table 2 also shows correlation of mode shapes against EMA using MAC values. High correlation of mode shapes is observed for all modes for both ISMA using random impacts and ISMA with IMU with values greater than 0.91. However, since 3rd mode was not estimated in ISMA using random impacts, there is no MAC value for the 3rd mode. Moreover, Table 2 shows results of ISMA with APCID against EMA [18], an alternate approach used to make ISMA more efficient compared to ISMA using random impacts at the expense of portability by using fully automated impact device. It can be observed that all the 3 modes observed in EMA were also observed in ISMA with APCID with modal parameter accuracies and MAC values are comparable to ISMA with IMU. In fact, the damping values obtained from ISMA with IMU are a little better overall compared to ISMA with APCID.

3.3 ISMA at 30 Hz running frequency with random impacts and semi-automated impact device

ISMA using random impacts was performed at 30 Hz running frequency with 20 averages. The resulting FRF is shown in Fig. 18.

Figure 18 shows high amplitude peaks at 30 Hz due to cyclic load component still present after 20 averages. While first 2 modes are present at 10.97 Hz and 14.9 Hz, the less sensitive 3rd mode cannot be observed as it is covered up by the cyclic load component.

ISMA was performed at 30 Hz using semi-automated impact device, (i.e., ISMA with IMU). The resulting FRFs at 1st average, 4 averages and 10 averages are shown in Fig. 19, 20 and 21, respectively.

Figure 19 shows the FRF at the start of the test where 1st and 2nd modes can be observed but 3rd mode is covered by the high peaks at 30 Hz due to cyclic load component. Figure 20 shows the FRF after 4 averages and it can be observed that the cyclic load component has been reduced significantly in just 4 averages from 2.4 m/s²N to 0.35 m/s²N with 85.4% suppression and the 3rd mode is starting to show up as the cyclic load component is suppressed. Figure 21 shows the FRF after 10 averages and it can be observed that

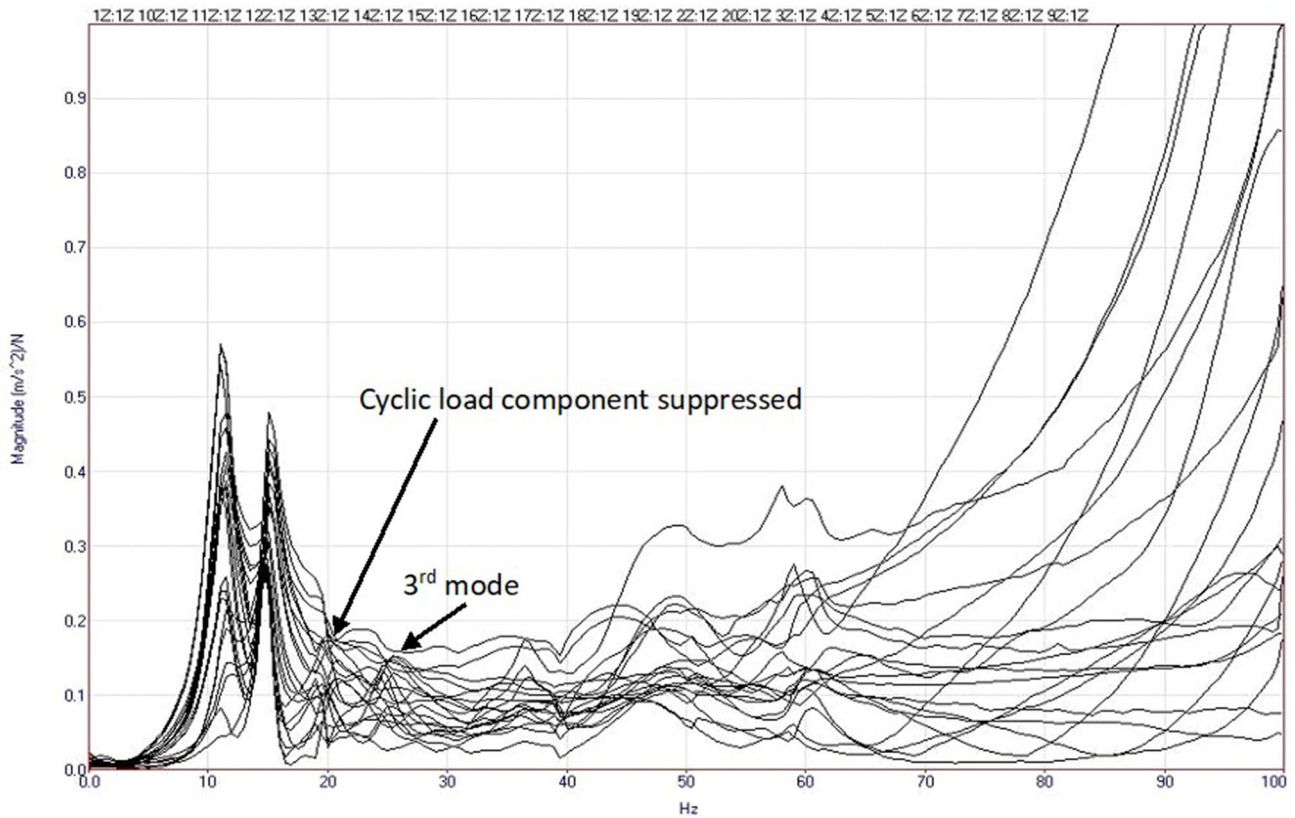


Fig. 14 FRF estimation for ISMA using IMU at 20 Hz (10 averages)

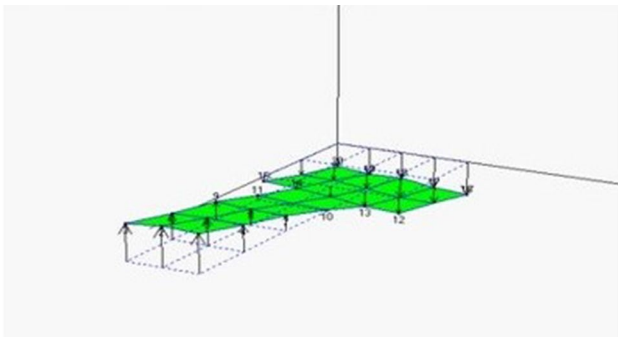


Fig. 15 Semi-automated Impact device 1st mode at 20 Hz

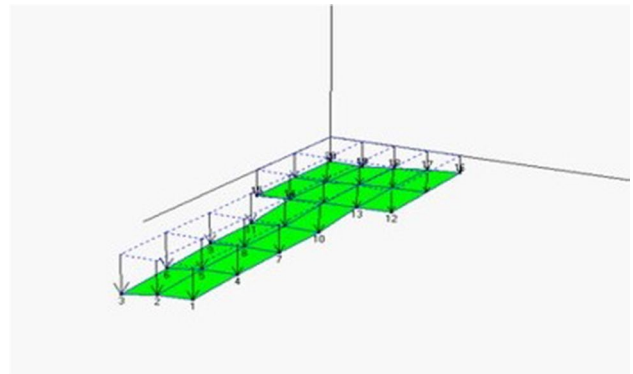


Fig. 16 Semi-automated Impact device 2nd mode at 20 Hz

cyclic load component is almost removed with 92.5% suppression (reduction from $2.05 \text{ m/s}^2\text{N}$ to $0.18 \text{ m/s}^2\text{N}$), and the 3rd mode can be observed clearly. From Fig. 21, 3 modes can be observed at 11.18 Hz, 14.95 Hz and 25.15 Hz similar to EMA. From Figs. 18 and 20, it can be observed that the cyclic load component is significantly suppressed with just 4 averages using semi-automated impact device compared to ISMA using random impacts for 20 averages. Mode shapes

obtained from semi-automated impact device at 30 Hz after 10 averages are shown in Figs. 22, 23 and 24.

From Figs. 22, 23 and 24, it can be observed that 1st mode shape is pitching, 2nd mode shape is heaving and 3rd mode shape is rolling, similar to the benchmark EMA.

Summary and comparison of the modal parameters extracted from Benchmark EMA, ISMA using random impacts at 30 Hz, semi-automated impact device at 30 Hz

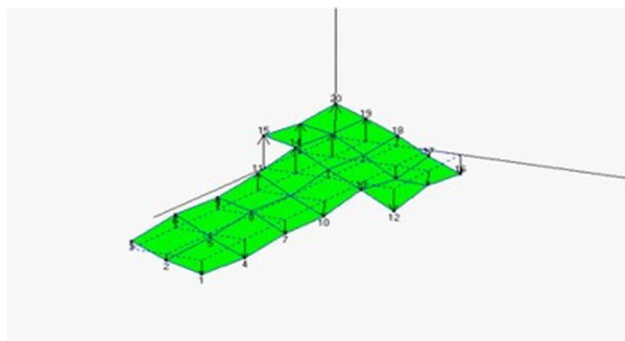


Fig. 17 Semi-automated Impact device 3rd mode at 20 Hz

and ISMA with APCID [18] at 30 Hz is given in Tables 3 and 4.

Natural frequencies and damping values of the modes estimated in EMA, ISMA using random impacts and ISMA with IMU, (i.e., semi-automated impact device) at 30 Hz running frequency are given in Table 3. Comparison of the modal parameters with the benchmark EMA in terms of percentage difference and Modal Assurance Criterion (MAC) values of ISMA using random impacts, ISMA with IMU and ISMA with APCID [18] at 30 Hz is given in Table 4. From Table 4 it can be observed that all the modes estimated in EMA are also estimated in ISMA with IMU with less than 3% difference in natural frequencies and less than 8% difference in damping values for all modes. Similar to the results at 20 Hz, 1st and 2nd modes in ISMA using random impacts have natural frequencies close to EMA with no estimation of 3rd mode due to presence of large cyclic load component at 30 Hz. The damping value of the 2nd mode is close to EMA, but the damping value of the 1st mode shows

large deviation with a difference of around 23% compared to EMA. Correlation of the mode shapes compared to EMA is also given in Table 4 using MAC values. High correlation of mode shapes is observed for all modes for both ISMA using random impacts and ISMA with IMU with values greater than 0.95. However, there is no MAC value for 3rd mode in ISMA using random impacts since the 3rd mode was not estimated. Moreover, Table 4 shows results of ISMA with APCID against EMA [18]. It can be observed that all the 3 modes observed in EMA were also observed in ISMA with APCID with modal parameter accuracies and MAC values comparable to ISMA with IMU overall. However, similar to the results at 20 Hz, the damping values obtained from ISMA with IMU are a little better overall compared to ISMA with APCID.

3.4 Discussion

Overall, by using semi-automated impact device in performing ISMA, in-service modal analysis can be performed in a portable and user-friendly manner. The results have shown that just 4 averages can suppress the disturbances significantly and 10 averages are sufficient to eliminate the disturbances as the phase of disturbance changes by nearly 180 degrees for each average with respect to the impact, which makes this semi-automated impact device a viable option for in-service modal analysis. The less sensitive 3rd mode appeared with as low as 4 averages using this device compared to ISMA using random impacts where 3rd mode did not appear after 20 averages. The natural frequencies of the modes obtained are close to the benchmark EMA with less than 3% difference for all the modes. The damping values of the modes obtained are also similar to EMA; however, for 1st mode the difference in damping

Table 1 Summary of modal parameters extracted using Benchmark EMA (BM), ISMA using random Impacts (A), ISMA with IMU (B) at 20 Hz

Modes	Natural frequency (Hz)			Damping (%)		
	BM	A	B	BM	A	B
1	11.48	10.86	11.14	9.054	8.363	8.187
2	15.12	15.03	14.91	4.334	5.165	4.308
3	25.44	–	24.77	4.504	–	4.321

Table 2 Comparison of modal parameters extracted using Benchmark EMA (BM), ISMA using random Impacts (A), ISMA with IMU (B) and ISMA with APCID (C)[18] at 20 Hz

Modes	Difference (%)						MAC values		
	Natural frequency (Hz)			Damping			BM vs A	BM vs B	BM vs C [18]
	BM vs A	BM vs B	BM vs C [18]	BM vs A	BM vs B	BM vs C [18]			
1	5.4	2.96	3.67	7.63	9.57	3.71	0.937	0.989	0.988
2	0.59	1.38	0.60	19.17	0.6	23.93	0.952	0.984	0.976
3	–	2.63	0	–	4.06	15.83	–	0.915	0.964

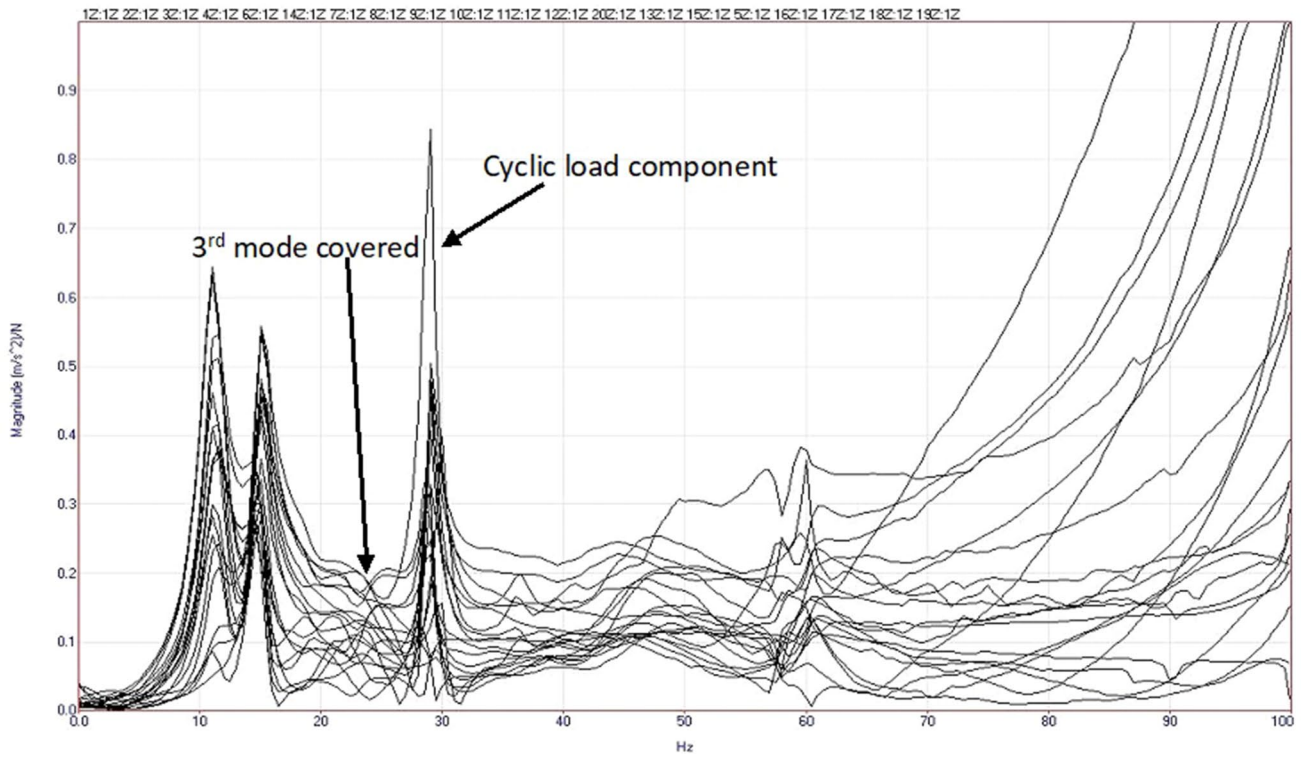


Fig. 18 FRF estimation for ISMA using random impacts at 30 Hz (20 averages)

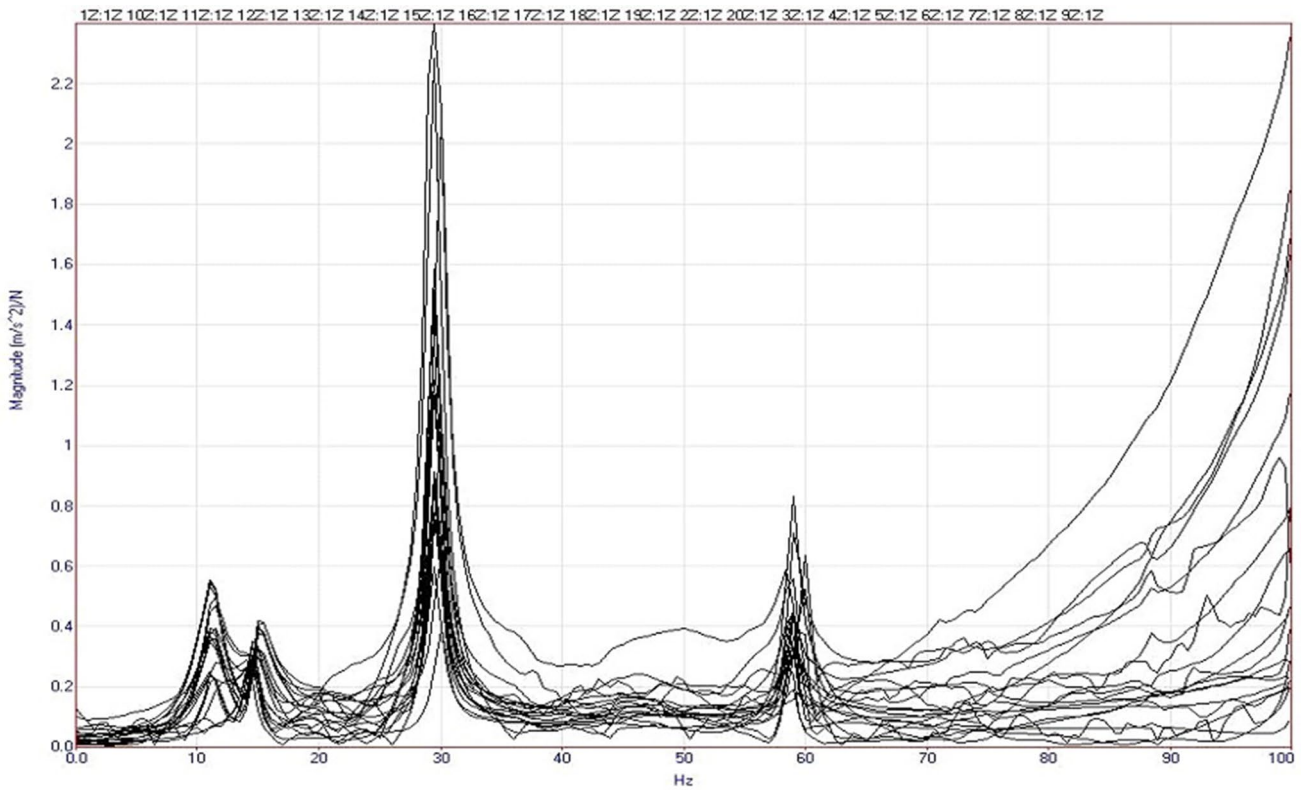


Fig. 19 FRF estimation for ISMA using IMU at 30 Hz (1st average)

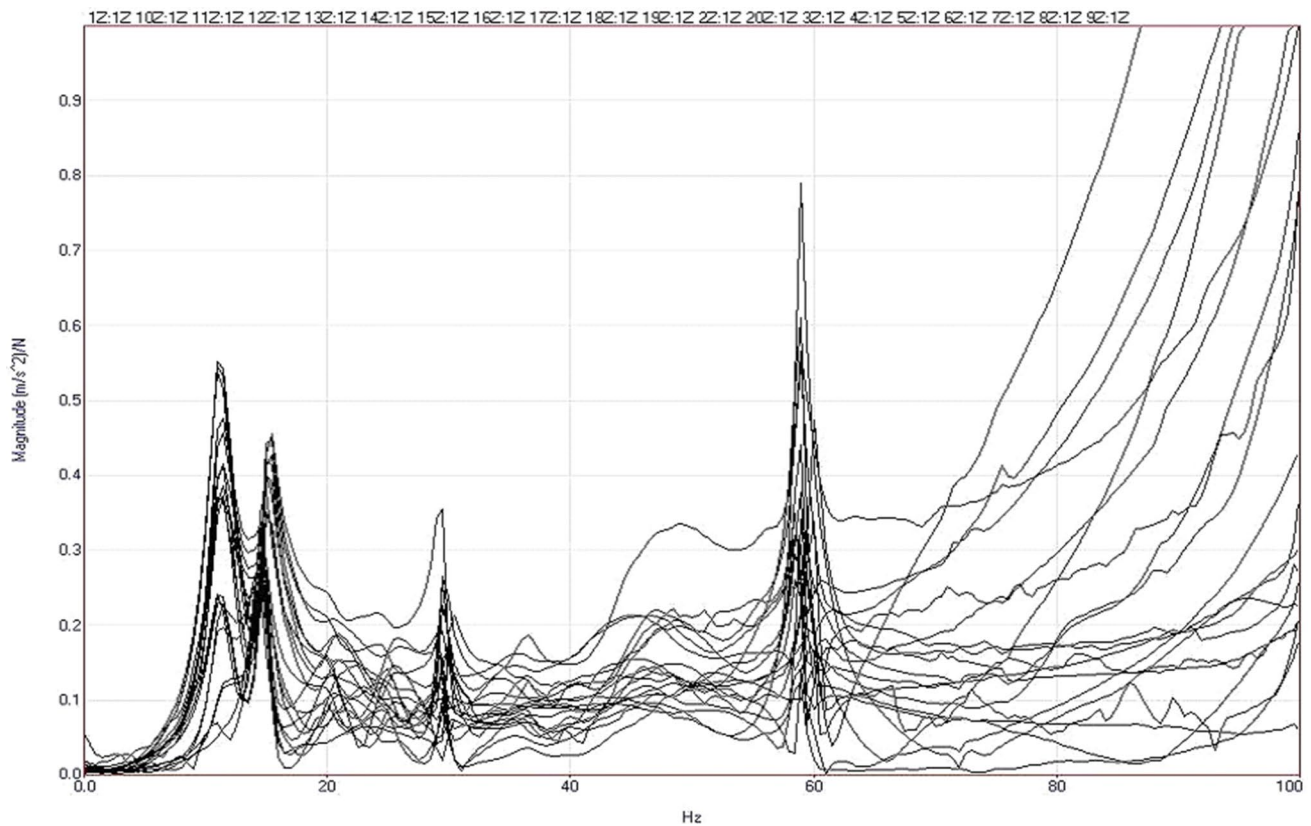


Fig. 20 FRF estimation for ISMA using IMU at 30 Hz (4 averages)

is more than 5% at both 20 Hz and 30 Hz motor running frequencies. The possible reason could be the changes in boundary condition of the test rig when the measurements were taken during operating condition [18]. The results show MAC values of greater than 0.9 for all modes at both 20 Hz and 30 Hz, which shows highly correlated and consistent mode shapes [31]. However, in ISMA using random impacts, there is no MAC value of 3rd mode since it could not be estimated at both 20 Hz and 30 Hz. While the MAC values for 1st and 2nd modes in ISMA using random impacts are greater than 0.9, they are less than their respective MAC values in ISMA with IMU tests at both 20 Hz and 30 Hz, which shows better correlation of mode shapes obtained for first 2 modes from ISMA with IMU compared to ISMA using random impacts.

Previously, a fully automated impact device called APCID was used to perform ISMA as an efficient alternative to ISMA using random impacts [18]. However, the efficiency of this device came at the expense of portability. In APCID, desired impact locations are determined automatically using Eq. (1) and then the structure is excited automatically without human intervention. The semi-automated device presented in this paper also determines desired impact location automatically using Eq. (1) but allows the human to excite

the structure manually to improve practicality of the device by removing actuator, its power supply and support structure of APCID. Using Eq. (1), the semi-automated device gives visual indication to the human to excite the structure and uses IMU with machine learning models to dynamically adjust T_{offset} in Eq. (1) to compensate for the randomness in human behaviour compared to consistent machine behaviour.

From Tables 2 and 4, it can be observed that the accuracy of the semi-automated impact device (i.e., ISMA with IMU) in terms of modal parameter estimation and MAC values is comparable to the fully automated impact device, (i.e., ISMA with APCID) with the advantage of better portability. In fact, overall accuracy of damping values of the semi-automated impact device is better than the fully automated impact device. The possible reason for this difference could be the manual application of ample force to excite all the modes properly in semi-automated impact device compared to a limited fixed force applied depending on the actuator and support structure, which may not excite all the modes properly. Another possible reason could be the change in testing and boundary conditions as the tests were performed at different times with different impact devices.

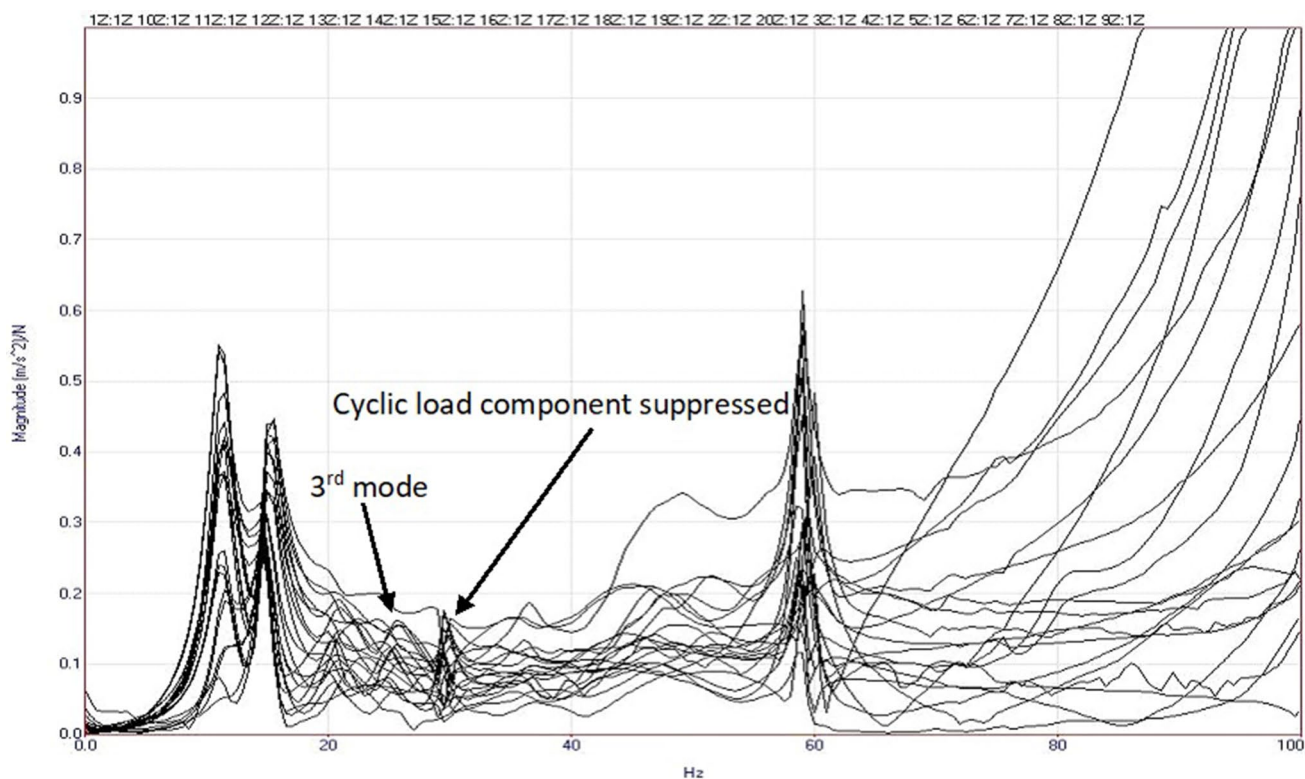


Fig. 21 FRF estimation for ISMA using IMU at 30 Hz (10 averages)

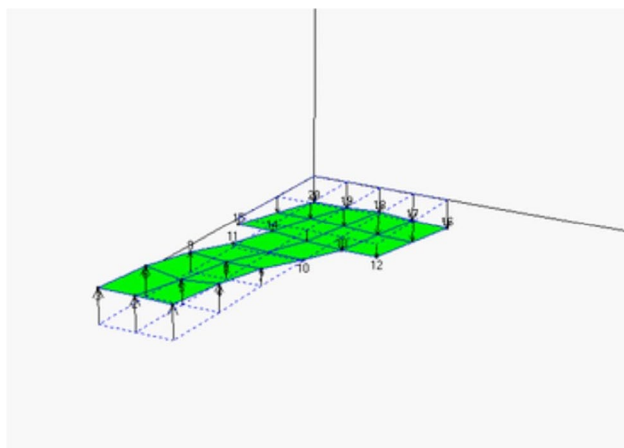


Fig. 22 Semi-automated impact device 1st mode at 30 Hz

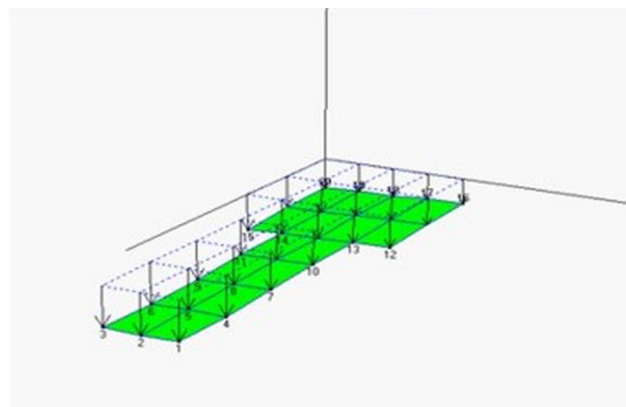


Fig. 23 Semi-automated impact device 2nd mode at 30 Hz

4 Conclusion

Lack of knowledge and control of impact with respect to the phase angle of the disturbance in ISMA using random impacts limited its practicality and effectiveness for in-service modal analysis as it required a large number of impacts. APCID was developed, which provided

knowledge and control of impact with respect to the phase angle of the disturbance. While this automated impact device was able to perform ISMA with minimum number of averages, its heavy weight and large size owing to its support structure made it unpractical for real life/industrial applications. APCID control scheme can be used with manual impacts but T_{offset} , (i.e., impact time) in APCID,

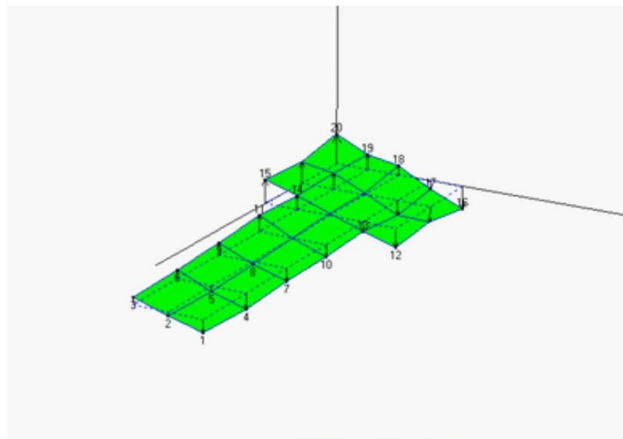


Fig. 24 Semi-automated impact device 3rd mode at 30 Hz

which is consistent with fully automated device, can vary depending on factors like reaction time, impact speed and type of impact owing to the randomness in human behaviour. Due to these variations, impacts cannot be imparted at desired locations, which makes the end product similar to ISMA using random impacts.

In this paper, a semi-automated impact device is used to perform ISMA in operating conditions. The device uses manual impacts for portability and practicality by avoiding bulky support structure of APCID, (i.e., fully automated

device), control scheme of APCID to get knowledge of impact with respect to the phase angle of the disturbance and IMU for development of machine learning models for physical human behaviour recognition, (i.e., prediction of impact time), making it user friendly by reducing the number of averages required to estimate modal parameters accurately.

The results showed that the semi-automated impact device estimated modal parameters accurately with less than 3% difference in natural frequencies and less than 10% difference in damping values compared to the benchmark EMA for all modes at 20 Hz and 30 Hz running frequencies, and cyclic load component was reduced by 91.2% and 92.5% at 20 Hz and 30 Hz, respectively. Good correlation of mode shapes with EMA was also found with MAC values of over 0.9 for all modes. The accuracy of the results of performing ISMA using semi-automated impact device is also comparable to the use of fully automated impact device, (i.e., ISMA with APCID) with overall better estimation of damping values while providing better portability.

From the results, it can be concluded that the proposed semi-automated impact device is a portable, user friendly and practical device and is a viable solution to perform in-service modal analysis with known input on mechanical structures.

Table 3 Summary of modal parameters extracted using Benchmark EMA (BM), ISMA using random Impacts (A), ISMA with IMU (B) at 30 Hz

Modes	Natural frequency (Hz)			Damping (%)		
	BM	A	B	BM	A	B
1	11.48	10.97	11.18	9.054	6.97	8.367
2	15.12	14.9	14.95	4.334	4.365	4.297
3	25.44	–	25.15	4.504	–	4.569

Table 4 Comparison of modal parameters extracted using Benchmark EMA (BM), ISMA using random Impacts (A), ISMA with IMU (B) and ISMA with APCID (C)[18] at 30 Hz

Modes	Difference (%)						MAC values		
	Natural frequency (Hz)			Damping					
	BM vs A	BM vs B	BM vs C [18]	BM vs A	BM vs B	BM vs C [18]	BM vs A	BM vs B	BM vs C [18]
1	4.44	2.61	4.59	23.02	7.59	0.24	0.954	0.991	0.988
2	1.45	1.12	1.2	0.71	0.85	14.86	0.982	0.991	0.97
3	–	1.14	0.44	–	1.44	6.24	–	0.978	0.98

Acknowledgements The authors wish to acknowledge the financial support and advice given by the Ministry of Higher Education for the Fundamental Research Grant Scheme (FRGS/1/2022/TK10/UM/02/29), private funding by SD Advance Engineering Sdn. Bhd. (PV032-2018) awarded to Zhi Chao Ong, Advanced Shock and Vibration Research (ASVR) Group of University of Malaya and other project collaborators.

Declarations

Conflict of interest The authors declare that they have no known competing financial interests or personal relationships that could have appeared to influence the work reported in this paper.

References

- Brandt A (2011) Noise and vibration analysis: signal analysis and experimental procedures. Wiley, Chichester
- Grosel J, Sawicki W, Pakos W (2014) Application of classical and operational modal analysis for examination of engineering structures. *Proc Eng* 91:136–141
- Gevinski JR, Pederiva R (2016) Prediction of dynamic strain using modal parameters. *J Braz Soc Mech Sci Eng* 38(1):49–57
- Siow PY et al (2021) Damage sensitive PCA-FRF feature in unsupervised machine learning for damage detection of plate-like structures. *Int J Struct Stab Dyn* 21(02):2150028
- Storti GC, da Silva Tuckmantel FW, Machado TH (2021) Modal parameters identification of a rotor-journal bearing system using operational modal analysis. *J Braz Soc Mech Sci Eng* 43(3):1–14
- Yu P, Chen G (2021) Nonlinear modal analysis and its application on prediction of resonance speed for a rotor–stator rubbing system. *J Braz Soc Mech Sci Eng* 43(4):1–20
- Rasmussen TØ, Santos IF (2021) Experimental & operational modal analysis applied to rotor-blade systems in a fully controlled testing environment. *J Braz Soc Mech Sci Eng* 43(10):1–10
- Brown DL et al (1979) Parameter estimation techniques for modal analysis. *SAE Trans* 88:828–846
- Brincker R, Zhang L, Andersen P (2001) Modal identification of output-only systems using frequency domain decomposition. *Smart Mater Struct* 10(3):441
- Zhang L, Brincker R, and Andersen P (2001) Modal indicators for operational modal identification. In: 19th international modal analysis conference (IMAC), Kissimmee, Florida
- Zahid FB, Ong ZC, Khoo SY (2020) A review of operational modal analysis techniques for in-service modal identification. *J Braz Soc Mech Sci Eng* 42(8):1–18
- Ong ZC (2013) Development of impact-synchronous modal analysis technique on motor-driven structure during operation. Universiti Malaya, Malaysia
- Rahman AGA, Chao OZ, Ismail Z (2011) Effectiveness of impact-synchronous time averaging in determination of dynamic characteristics of a rotor dynamic system. *Measurement* 44(1):34–45
- Rahman AGA, Ong ZC, Ismail Z (2011) Enhancement of coherence functions using time signals in modal analysis. *Measurement* 44(10):2112–2123
- Rahman A et al (2014) Enhancement of impact-synchronous modal analysis with number of averages. *J Vib Control* 20(11):1645–1655
- Ong ZC et al (2017) Assessment of the phase synchronization effect in modal testing during operation. *J Zhejiang Univ-Sci A* 18(2):92–105
- Lim HC (2018) Automated impact device based on phase synchronisation assessment for the enhancement of impact-synchronous modal analysis during operation. University of Malaya, Malaysia
- Lim HC, Ong ZC, Brandt A (2018) Implementation of phase controlled impact device for enhancement of frequency response function in operational modal testing. *J Franklin Inst* 355(1):291–313
- Lim HC et al (2019) A performance study of controlled impact timing on harmonics reduction in operational modal testing. *J Dyn Syst Meas Control*. Doi 10(1115/1):4041609
- Chao OZ et al. (2015) Experimental validation of phase synchronisation effects in optimising impact-synchronous time averaging. In: 6th international operational modal analysis conference (IOMAC 2015), Gijón, Spain
- Bangaru SS et al (2021) ANN-based automated scaffold builder activity recognition through wearable EMG and IMU sensors. *Autom Constr* 126:103653
- Wu Z et al (2019) Yoga posture recognition and quantitative evaluation with wearable sensors based on two-stage classifier and prior Bayesian network. *Sensors (Basel)* 19(23):5129
- Xing H et al (2017) Pedestrian stride length estimation from IMU measurements and ANN based algorithm. *J Sensors*. <https://doi.org/10.1155/2017/6091261>
- Zahid FB et al (2021) Inertial sensor based human behavior recognition in modal testing using machine learning approach. *Meas Sci Technol* 32(11):115905
- Ong ZC et al (2019) An inconsistent phase selection assessment for harmonic peaks elimination in operational modal testing. *Arch Appl Mech* 89(12):2415–2430
- Hamed M (2016) Characterisation of the dynamics of an automotive suspension system for on-line condition monitoring. University of Huddersfield, England
- Rouillard V, Lamb M (2020) Some characteristics of the heave, pitch and roll vibrations within urban delivery routes. *Pack Technol Sci* 33(3):113–121
- Tseng HE, Hrovat D (2015) State of the art survey: active and semi-active suspension control. *Veh Syst Dyn* 53(7):1034–1062
- Ibicek T, Thite AN (2012) Quantification of human discomfort in a vehicle using a four-post rig excitation. *J Low Freq Noise Vib Active Control* 31(1):29–42
- Ibicek T, Thite AN (2014) In situ measurement of discomfort curves for seated subjects in a car on the four-post rig. *Adv Acoust Vib*. <https://doi.org/10.1155/2014/239178>
- Pastor M, Binda M, Harčarik T (2012) Modal assurance criterion. *Proc Eng* 48:543–548

Publisher's Note Springer Nature remains neutral with regard to jurisdictional claims in published maps and institutional affiliations.

Springer Nature or its licensor (e.g. a society or other partner) holds exclusive rights to this article under a publishing agreement with the author(s) or other rightsholder(s); author self-archiving of the accepted manuscript version of this article is solely governed by the terms of such publishing agreement and applicable law.